

EFFECT OF A STELLAR COMPANION ON THE MODELING OF HD 142527 INFRARED SED

Erick Nagel

Departamento de Astronomía
Universidad de Guanajuato, Mexico

Received 2013 August 5; accepted 2013 October 17

RESUMEN

El descubrimiento de una compañera de la estrella Herbig Ae/Be HD 142527 motiva el estudio del efecto que produce en la SED. El principal cambio en la configuración del sistema es la formación de una brecha en el disco. Debido a este cambio se forma una pared (lado externo del hueco), la cual está iluminada frontalmente por la radiación estelar. Se modela la SED, considerando todas las componentes: un disco con dos brechas (una producida por la compañera estelar y la otra por planetas potenciales), tres paredes (dos asociadas con las brechas y la otra por sublimación de polvo), y corrientes de material ópticamente delgadas en las brechas y las estrellas. El material ópticamente delgado requerido para ajustar el espectro está localizado en un halo, pero también dentro de las brechas. El halo modelado es más pequeño que el considerado en un modelo previo del sistema.

ABSTRACT

The discovery of a companion of the Herbig Ae/Be star HD 142527 motivates the study of the effect that it produces on the SED. The main change on the system configuration is the formation of a gap in the disk. Due to this change, a wall (outer edge of the gap), which is frontally illuminated by stellar radiation is formed. We present a model for the SED, considering all the components: a disk with two gaps (one produced by the stellar companion and the other by potential planets), three walls (two associated with the gaps and the other with dust sublimation), and optically thin streams of material in the gaps and the stars. The optically thin material required to fit the spectrum is located in a halo, but also inside the gaps. The modeled halo is smaller than the one considered in a previous model of the system.

Key Words: infrared: general — protoplanetary disks — stars: pre-main sequence

1. INTRODUCTION

Disks around stellar systems are a ubiquitous feature of the initial stage in the life of stars. Along with this, the paradigm of planet formation requires such a system. This has led researchers in the last decades to a strong effort in understanding the processes leading to the formation of planetary systems in disks (Greenberg et al. 1978; Wetherill 1980; Lissauer 1993; Pollack et al. 1996; Ida & Lin 2004). There are several direct and indirect ways to detect the presence of planets. In the former category, there is the detection by transits (Lissauer et al. 2011; Holman et al. 2010) and in the latter is the modeling of SEDs (D’Alessio et al. 2005; Nagel et al. 2010, 2012;

Espaillet et al. 2007, 2008, 2011). In this work, we concentrate on the latter, complementing it with information extracted from images, where there is no direct evidence of a planet. The general idea behind this is that a planet or star is able to sweep material around its orbit, forming gaps or even holes (Zhu et al. 2011; Quillen et al. 2004; Rice et al. 2006). There are images of gaps where the evidence suggests that they are formed by planets (Thalmann et al. 2010), but in many cases, we depend on the modeling of the SED.

The HD 142527 stellar system has been previously modeled using a disk with a gap assumed to be formed by a planet (Verhoeff et al. 2011). The detec-

tion of a possible stellar companion for this system (Biller et al. 2012) motivates us to revisit the modeling of this system. A model consistent with a stellar companion would be helpful in the future, in order to pursue a study of the possible configurations of planets or lower mass stars responsible for the total shaping of the system. The paper is organized as follows. In § 2, we summarize the relevant observations of HD 142527. § 3 is devoted to previous models as well as to a new model of this system. In § 4, we discuss the modeling results. Finally, conclusions are presented in § 5.

2. OBSERVATIONS

The Herbig Ae star HD 142527 is associated with the Sco OB2-2 star formation region, thus, we adopt a distance of $d = 145$ pc to this system (de Zeeuw et al. 1999). This stellar system was imaged in the near-infrared by Fukagawa et al. (2006). In their observation, two bright arcs opposite to one another and a spiral arm are clearly seen. This observation is complemented with mid-infrared images of the same system by Fujiwara et al. (2006), where arc-like emission on the outer disk is also present. Fukagawa et al. (2006) suggest that a companion is responsible for these features. Additionally, Fujiwara et al. (2006) suggest that the part of the inner rim of the outer inclined disk, which is located along the line of sight, explains the opposite arcs that are observed. More recently, Casassus et al. (2012) imaged the outer regions of HD 142527 with the NICI camera on Gemini South. The image shows that the outer boundary of the gap is composed of various spiral arms. This result suggests the presence of a companion (probably a planet) shaping the gap. A structure of many spiral arms is confirmed by Rameau et al. (2012). The observation that motivates this work was done by Biller et al. (2012). Biller et al. (2012) uses NACO at VLT to interpret an asymmetry in the flux as a stellar companion of $\sim 0.1 - 0.4 M_{\odot}$. The estimated semimajor axis is 14_{-5}^{+12} au. Biller et al. (2012) also suggested that in this scenario the surroundings of the secondary are heated, which explains the emission in the L band.

3. MODELING OF THE HD 142527 SED

3.1. Previous modeling

The observations described in § 2, represent the constraints used for the modeling of the HD 142527 stellar system. The arcs observed by Fukagawa et al. (2006) and Fujiwara et al. (2006) correspond to the emission of the outer rim of the gap. Verhoeff et al. (2011) take this into account for the modeling of the HD 142527 stellar system. In that work,

photometric data from the optical to the millimetric and infrared images are consistently modeled. The model of Verhoeff et al. (2011) consists of three main components. The first one is a small inner disk with inner and outer radii of 0.3 and 30 au, respectively. This disk has a puffed-up inner rim which shadows part of its inner zones. The second component is an optically thin spherical halo with a 30 au radius. Finally, the last component is a massive outer disk starting at 130 au and ending at 200 au with a very high inner wall. The inclination taken is $i = 20^{\circ}$. A 60 au wall is necessary to explain the large IR excess as noted by Verhoeff et al. (2011).

The spiral arms structure observed by Rameau et al. (2012) and Casassus et al. (2012) suggests the presence of planets or a very low-mass star in the gap. In the modeling, details of this structure are not taken into account. This leaves the conclusions in Verhoeff et al. (2011) unaltered, because their contribution to the SED is not the main one.

3.2. New modeling

The HD 142527 data used for the fitting are photometric fluxes presented by Verhoeff et al. (2011) in their Table 5 and the low resolution Spitzer-IRS spectrum taken from Figures 7 and 11 of Juhász et al. (2010). The parameters of the primary star come from Verhoeff et al. (2011). For the mass accretion rate on the secondary star the typical value for low-mass stars given in Gullbring et al. (1998) is considered.

As noted in § 2, Biller et al. (2012) argue in favor of a companion to the Herbig Ae star. This star is located inside the inner disk modeled by Verhoeff et al. (2011). We have considered this fact as our motivation to find a new model consistent with the companion. For this model, the secondary star carves a gap in the inner disk (Nelson et al. 2000). The SED of the disk is calculated using the model of a passive irradiated circumstellar disk around a Herbig Ae star by Dullemond, Dominik, & Natta (2001).

Inside the gap, there is optically thin material that connects the outer disk with the outer part of the inner disk (Artymowicz & Lubow 1996). The modeling of the gap is done in 3 steps; in the first one, we eliminated the disk emission coming from the region between the inner and the outer radii of the gap; in the second step we included the emission of the outer rim using the formalism previously described in D'Alessio et al. (2005) and Nagel et al. (2010); finally, the emission of optically thin material in the gap is calculated as in Nagel et al. (2012).

TABLE 1

MAIN PARAMETERS OF THE MODEL

Parameter	
$M_{\star,\text{primary}}$	$2.2 M_{\odot}$
$R_{\star,\text{primary}}$	$3.8 R_{\odot}$
$T_{\star,\text{primary}}$	6250 K
$\dot{M}_{\star,\text{primary}}$	$2 \times 10^{-7} M_{\odot} \text{ yr}^{-1}$
$\dot{M}_{\star,\text{secondary}}$	$3.25 \times 10^{-8} M_{\odot} \text{ yr}^{-1}$
d	145 pc
i	20°
$R_{\text{min,disk}}$	0.467 au
$R_{\text{max,disk}}$	200 au

As in the previous modeling (see § 3.1), the structure of our system includes a large gap between 30 and 130 au (see Table 1 for the main parameters used in our model) probably formed by one or more planets. Casassus et al. (2012) develop a hydrodynamical simulation in order to conclude that a circular planet at 90 au is able to carve the disk up to 130 au. In order to model the SED, we included the emission of the outer rim, and the emission of optically thin dust inside the gap, consistent with a planet at 90 au, in the way described in Nagel et al. (2012). From preliminary modeling of the latter, we concluded that the material is cold enough to produce the silicate features in the mid-infrared, thus, it is not important for the fitting of the bands, but it is to fit larger wavelengths. The importance of including the material in the gap is highlighted by Verhoeff et al. (2011), looking at a brightness radial profile (see their Figure 7) that they were not able to fit. Also, the observations of Casassus et al. (2013) suggest the existence of this material. A sketch of the system modeled here is presented in Figure 1.

To avoid starting from scratch, we based our model on the basic picture of Verhoeff et al. (2011). The size of the inner and outer disks, the location and height of the inner rim of the outer disk, all are taken from Verhoeff et al. (2011). We include amorphous carbon as a source of a continuous opacity (Mathis & Whiffen 1989, for the optical properties), which is required for the millimeter range modeling. The abundance ratio between silicates and carbon is considered as in Verhoeff et al. (2011). Modeling the $10 \mu\text{m}$ feature depends on the silicates composition. Van Boekel et al. (2005) fitted the band and found the silicates composition for HD 142527. This grain composition is taken by Verhoeff et al.

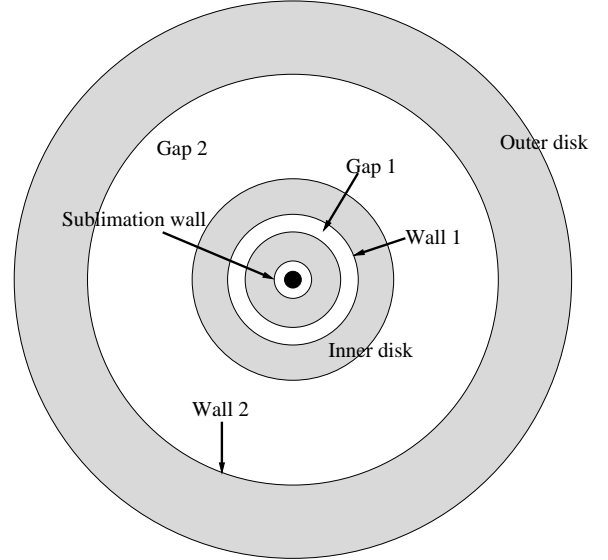


Fig. 1. Sketch of the geometrical model used. The structure of the disk is shown pole on. Besides, inside the gaps, there is optically thin material that connects the companion star and planet with the inner and outer parts of the disk. Also, some optically thin material is located in a spherical structure (halo), which has not been presented in the diagram to avoid confusion. The components are not shown to scale.

(2011). We take the two most abundant species for this work: large grains ($1.5 \mu\text{m}$) made of pyroxene ($\text{Mg}_{0.8}\text{Fe}_{0.2}\text{SiO}_3$) and enstatite (MgSiO_3). The optical properties of pyroxene and enstatite are given in Dorschner et al. (1995) and Jäger et al. (1998), respectively. The less abundant species (forsterite and silica) are not considered. Because our aim is to construct a model that will be consistent with a particular geometrical distribution of dust, this assumption will not modify our main conclusions.

The gap carved by the companion defines the circumprimary and circumbinary disks. The outer radius of the circumprimary disk is estimated using the analytical approach developed by Nagel & Pichardo (2008) for circular binaries. We calculate the inner radius of the circumbinary disk using the fit given in equation (6) in Pichardo, Sparke, & Aguilar (2008). For the mass of the secondary star associated to the fit, we choose the two cases that were used for the modeling, we choose the range limits considered by Biller et al. (2012): $0.1, 0.4 M_{\odot}$. The stellar parameters are given in Table 2 using the PMS tracks of Siess, Dufour, & Forestini (2000).

The inner radius of the disk is $R_{\text{min,disk}}$, which refers to the location of the sublimation wall. In order to calculate the emission of this wall, we con-

TABLE 2
PARAMETERS OF THE SECONDARY STAR

Case	1	2
$M_{\star, \text{secondary}}$	$0.1 M_{\odot}$	$0.4 M_{\odot}$
$R_{\star, \text{secondary}}$	$0.85 R_{\odot}$	$0.66 R_{\odot}$
$T_{\star, \text{secondary}}$	2998 K	3464 K

TABLE 3
PARAMETERS OF THE WALLS

Wall due to	R_{min} (au)	R_{wall} (au)	Height (au)
Sublimation	0.271 ^a	0.467	0.011
$0.1 M_{\odot}$ Secondary	—	21.79	0.23
$0.4 M_{\odot}$ Secondary	—	22.997	0.236
Planet(s)	—	130	46

^aFor the wall due to sublimation, there is a minimum radius (R_{min}) because the wall is curved.

sider that the wall is curved due to the dependency of sublimation temperature on density (Isella & Natta 2005; Nagel et al. 2013) and due to the settling, because at the same location, the temperature is lower for larger grains (Tannirkulam, Harries, & Monnier 2007). The sublimation wall emission is calculated using the code described in Nagel et al. (2013), but including the settling. We take the parameter ϵ to characterize the degree of sedimentation, and choose $\epsilon = 0.01$ as typical (D’Alessio et al. 2006). Associated to the two gaps, there are two walls which are directly illuminated by the stars. In the inner wall, the heating due to the primary and secondary stars is considered as in Nagel et al. (2010); for the outer wall, we consider that the heating by the secondary star and planet(s) is not important. However, the shadowing of the primary star radiation by the circumprimary disk for the former and by the inner wall of the circumbinary disk for the latter is taken into account as in Espaillat et al. (2010). The height of the walls is calculated using the model of circumstellar disks described in Dullemond et al. (2001). This value depends on the disk density, which is also adjusted to explain the peak at $40 \mu\text{m}$. For the fitting, the height of the wall should be 46 au compared to the value of 60 au coming from Verhoeff et al. (2011). Table 3 shows a summary of the parameters associated to the walls.

As noted, the modeling of the dust emission in both gaps is done as in Nagel et al. (2012). The material is located in streams that connect the outer rim

TABLE 4
PARAMETERS OF THE GAPS

	R_{int} (au)	R_{ext} (au)	M_{thin} (M_{\odot}) ^a
Inner gap			
Case 1	6.8135	21.79	3.52×10^{-12}
Case 2	5.525	22.997	2.23×10^{-12}
Outer gap			
Case 1	30	130	8.88×10^{-8}
Case 2	30	130	8.22×10^{-8}

^a M_{thin} corresponds to the mass of the optically thin material in the gap.

of the gap with the secondary object: a star in the inner and a planet in the outer gap. Also, there are streams connecting this object and the inner zones of the disk. Some evidence of an asymmetric configuration comes from the observation of one bright spiral arm and several dimmer ones by Rameau et al. (2012); their location could represent the launching point of the previously mentioned streams. Due to the many parameters considered in this modeling, including the detailed structure of the material in the gaps suggested by Fukagawa et al. (2006), Fujiwara et al. (2006), Rameau et al. (2012), and Casassus et al. (2012) will not restrict such structure; thus, the broad conclusions of the paper remain unaltered.

The emission from the stars, and the disk with gaps (including the walls), gives us a spectrum resembling the observed one. Starting from this fit, the amount of optically thin material located in both gaps and in a spherical halo around the central star is adjusted, in order to find the best fit. From the fitting of the SED, the mass in dust located in the inner and outer gaps is 3.52×10^{-12} (2.23×10^{-12}) and 8.88×10^{-8} (8.22×10^{-8}) M_{\odot} , for cases 1 and 2, respectively. The parameters for the gaps are given in Table 4. The emission coming from the halo is calculated with the same code used to calculate the spectrum of the streams, but adapted to the new configuration. The halo mass is $4.07 \times 10^{-12} M_{\odot}$. The modeled SED for a 0.1 and a $0.4 M_{\odot}$ secondary star is given in Figures 2 and 3, respectively.

4. DISCUSSION

From the images of HD 142527 in Casassus et al. (2013) and from the modeling of this system by Verhoeff et al. (2011), we recognize that the gap tentatively formed by one or more planets is filled

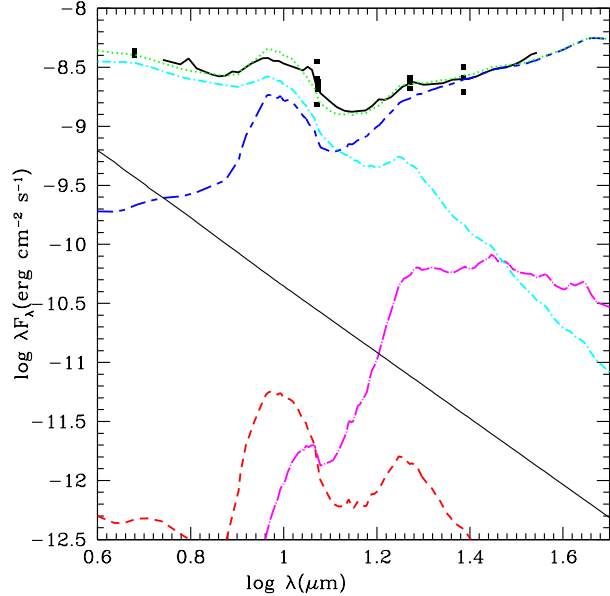


Fig. 2. Spectrum of the stellar system HD 142527 for a $0.1 M_{\odot}$ secondary star. The Spitzer spectrum is represented with a solid line. The squares define the photometric fluxes (taken with errors from Verhoeff et al. 2011). For the model, the emission from the stars is given as a thin solid line. The spectrum of the disk (including the walls) is represented by a short-long-dashed line. The optically thin material is distributed in 3 parts: in the gap carved by the secondary star (dashed line), in the gap carved by the planet(s) (dot-long-dashed line) and in a spherical halo around the primary star (dot-dashed line). The model fit is given by a dotted line.

with some amount of material. A detailed characterization of the distribution of material inside this gap is not known, because we do not know the orbital parameter(s) of the planet(s) located inside the gap. For our analysis we considered the orbital parameters of the hypothetical planet that forms the gap, according to Casassus et al. (2012). The general picture is that in the gap a stream of material connects the outer disk with the planet and a second stream connects the latter with the inner disk (Kley, D’Angelo, & Henning 2001). This is a simplified version of what is really happening inside the gap, because it is not able to explain the location of the inner edge of the gap (Casassus et al. 2012). Following this fact, there is a possibility that there are one or more planets closer to the star, which are responsible for placing the inner edge at the right position. Looking at this realistic scenario, the pattern for the material in the gap is more complicated than the simple picture presented here. However, we do not deny the importance of this element for a

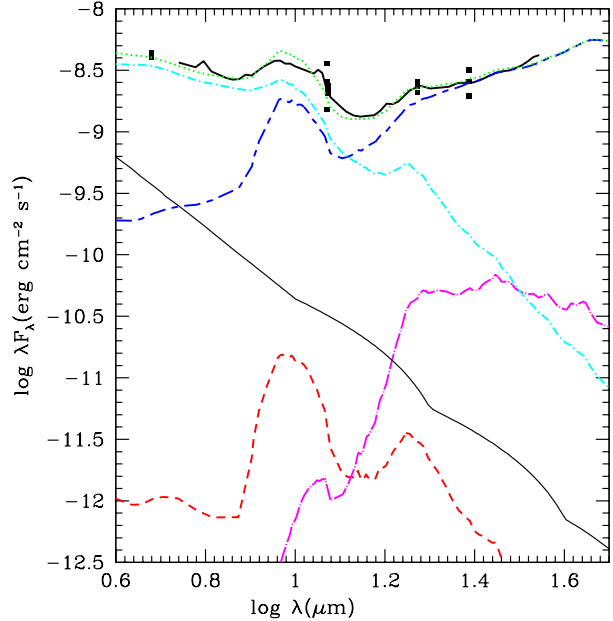


Fig. 3. Spectrum of the stellar system HD 142527 for a $0.4 M_{\odot}$ secondary star. The meaning of the different lines is the same as in Figure 2.

more detailed modeling of the system, when future observational restrictions are available.

For the fitting of the short wavelength regime, and in particular for the silicate bands fit, the material in the inner region of the disk is hot enough to produce this emission. The dust inside the outer gap has a negligible contribution to the silicates features and mainly contributes at wavelengths longer than $20 \mu\text{m}$.

At wavelengths longer than $20 \mu\text{m}$, the main contribution for the spectrum comes from the cold outer disk, including the wall located in the inner rim. The peak at $\lambda = 40 \mu\text{m}$ is explained with an outer disk with a mass smaller than that of the disk in Verhoeff et al. (2011). The material in the outer gap has a small contribution in the SED, but its presence is required as noted in Verhoeff et al. (2011) (see Section 3.2) and more recently by Casassus et al. (2013). They report CO(3-2) line emission inside the outer gap, which can explain flow rates of gas up to $2 \times 10^{-7} M_{\odot} \text{ yr}^{-1}$, a value consistent with the actual estimated rate onto the star. One assumes that there is dust immersed in the streams of gas, which is responsible for the small amount of gap emission. Note that another reason why a large SED contribution of this region cannot be expected is that according to our model this is a site of planet formation. In such a region, a considerable amount of dust is

located in grains with large sizes, such as protoplanets and planetesimals, as opposed to micron-sized grains, where the observed emission comes from.

5. SUMMARY AND CONCLUSIONS

The model of Verhoeff et al. (2011) for the SED of the HD 142527 stellar system is considered as a starting point for a new model. This new model includes the contribution of optically thin material in an inner gap formed by a companion star (Artymowicz & Lubow 1994), and also inside the outer gap formed by planet(s) (Rice et al. 2006). As in the previous model, there is dust in a halo. The SED fitting with the new distribution of optically thin dust leads to a halo that shrinks in size from 30 au (the previous modeling) to 5 au. Note that Verhoeff et al. (2011) comment that the outer radius of the halo is not constrained by the observations. When new observations that restrict the halo size become available, they will provide a valuable test of our model.

The mass of dust in the inner and outer gap is 3.52×10^{-12} (2.23×10^{-12}) and 8.88×10^{-8} (8.22×10^{-8}) M_{\odot} , for cases 1 and 2, respectively. For a gas to dust mass ratio of 100, the mean gas surface density in the inner and outer gap are $\Sigma_{\text{inner gap}} = 2.34 \times 10^{-6}$ ($\Sigma_{\text{inner gap}} = 1.28 \times 10^{-6} \text{ g cm}^{-2}$) and $\Sigma_{\text{outer gap}} = 1.58 \times 10^{-3}$ ($\Sigma_{\text{outer gap}} = 1.46 \times 10^{-3} \text{ g cm}^{-2}$), for cases 1 and 2, respectively. These values are divided by the non-perturbed disk density $\Sigma_{\text{disk}} = 8 \times 10^{-4}$ and $\Sigma_{\text{disk}} = 3.75 \text{ g cm}^{-2}$ to find the gap to disk surface density ratio, for the inner and outer gap, respectively. These ratios are 2.92×10^{-3} (1.59×10^{-3}) and 4.22×10^{-4} (3.91×10^{-4}) for the inner and outer gap, for cases 1 and 2, respectively. These values can be compared to the simulations of a Jupiter mass planet immersed in a disk. Results by Crida, Morbidelli, & Masset (2006) show that for low viscosities this ratio is around 0.1. Thus, one can conclude that the outer gap that we assume is carved by planets requires another mechanisms to get rid of gap material, such as mass accretion by planets. Noteworthy, for the inner gap, the estimated ratio is consistent with the fact that for an immersed 0.1 or $0.4 M_{\odot}$ star, it is expected that this ratio is orders of magnitude lower with respect to a gap shaped by an immersed Jupiter mass planet.

The halo mass is $4.07 \times 10^{-12} M_{\odot}$, considerably lower than the amount registered in the halo of Verhoeff et al.'s (2011) model, because of its smaller size. As pointed out by Verhoeff et al. (2011), an extended halo of dust is not easy to obtain. A possible mechanism is dynamical excitation of planetesimals by an inwardly migrating planet (Krijt & Do-

minik 2011). For a 3-planet system, the interaction with an outer disk of planetesimals results in clouds with a 100 – 1000 au radius (Raymond & Armitage 2013). Stirring the material up to a height of 5 au (this model) requires a weaker interaction with planets than the excitation required to produce a 30 au halo (Verhoeff et al.'s 2011 model). Thus, a highlight of this work is that the new halo configuration is easier to explain. However, it is important to emphasize that the size of the halo is not consistently calculated with a simulation of the interaction of the bodies in the system with the gaseous-dusty structure. An analysis of this mechanism should be considered in the future.

As a final remark, we were able to find a successful model for the SED of HD 142527, that includes a secondary star (Biller et al. 2012) which carves a gap in the inner disk. This is a first step in the process of building a model that includes details of the disk structure (Casassus et al. 2013) as well as the patterns of the material inside the gaps. In order to address the latter it is important for future research, to run hydrodynamical simulations of planetary systems immersed in a disk (Zhu et al. 2011), since a by-product these will allow to explain the thickness of the outer gap in this system.

The author thanks the staff of the Department of Astronomy of the University of Guanajuato for their continuous support during the development of this work, and Dra. Cynthia Montaudon Tomas of the DAIP also from the University of Guanajuato for a critical reading of the original version of the paper.

REFERENCES

- Artymowicz, P., & Lubow, S. H. 1994, *ApJ*, 421, 651
 _____ . 1996, *ApJ*, 467, L77
 Biller, B., et al. 2012, *ApJ*, 753, L38
 Casassus, S., et al. 2012, *ApJ*, 754, L31
 Casassus, S., et al. 2013, *Nature*, 493, 191
 Crida, A., Morbidelli, A., & Masset, F. 2006, *Icarus*, 181, 587
 D'Alessio, P., Calvet, N., Hartmann, L., Franco-Hernández, R., & Servín, H. 2006, *ApJ*, 638, 314
 D'Alessio, P., et al. 2005, *ApJ*, 621, 461
 de Zeeuw, P. T., Hoogerwerf, R., de Bruijne, J. H. J., Brown, A. G. A., & Blaauw, A. 1999, *AJ*, 117, 354
 Dorschner, J., Begemann, B., Henning, T., Jäger, C., & Mutschke, H. 1995, *A&A*, 300, 503
 Dullemond, C. P., Dominik, C., & Natta, A. 2001, *ApJ*, 560, 957
 Espaillat, C., Calvet, N., Luhman, K. L., Muzerolle, J., & D'Alessio, P. 2008, *ApJ*, 682, L125

- Espaillat, C., et al. 2007, *ApJ*, 670, L135
 Espaillat, C., et al. 2010, *ApJ*, 717, 441
 Espaillat, C., et al. 2011, *ApJ*, 728, 49
 Fujiwara, H., et al. 2006, *ApJ*, 644, L133
 Fukagawa, M., et al. 2006, *ApJ*, 636, L153
 Greenberg, R., Hartmann, W. K., Chapman, C. R., & Wacker, J. F. 1978, *Icarus*, 35, 1
 Gullbring, E., Hartmann, L., Briceño, C., & Calvet, N. 1998, *ApJ*, 492, 323
 Holman, M. J., et al. 2010, *Science*, 330, 51
 Ida, S., & Lin, D.N.C. 2004, *ApJ*, 604, 388
 Isella, A., & Natta, A. 2005, *A&A*, 438, 899
 Jäger, C., Molster, F. J., Dorschner, J., Henning, Th., Mutschke, H., & Waters, L. B. F. M. 1998, *A&A*, 339, 904
 Juhász, A., et al. 2010, *ApJ*, 721, 431
 Kley, W., D'Angelo, G., & Henning, T. 2001, *ApJ*, 547, 457
 Krijt, S., & Dominik, C. 2011, *A&A*, 531, 80
 Lissauer, J. J. 1993, *ARA&A*, 31, 129
 Lissauer, J. J., et al. 2011, *Nature*, 470, 53
 Mathis, J. S., & Whiffen, G. 1989, *ApJ*, 341, 808
 Nagel, E., D'Alessio, P., Calvet, N., Espaillat, C., Sargent, B., Hernández, J., & Forrest, W. J. 2010, *ApJ*, 708, 38
 Nagel, E., D'Alessio, P., Calvet, N., Espaillat, C., & Trinidad, M. A. 2013, *RevMexAA*, 49, 43
 Nagel, E., Espaillat, C., D'Alessio, P., & Calvet, N. 2012, *ApJ*, 747, 139
 Nagel, E., & Pichardo, B. 2008, *MNRAS*, 384, 548
 Nelson, R. P., Papaloizou, J. C. B., Masset, F., & Kley, W. 2000, *MNRAS*, 318, 18
 Pichardo, B., Sparke, L. S., & Aguilar, L. A. 2008, *MNRAS*, 391, 815
 Pollack, J. B., Hubickyj, O., Bodenheimer, P., Lissauer, J. J., Podolak, M., & Greenzweig, Y. 1996, *Icarus*, 124, 62
 Quillen, A. C., Blackman, E. G., Frank, A., & Varniere, P. 2004, *ApJ*, 612, L137
 Rameau, J., Chauvin, G., Lagrange, A. -M., Thebault, P., Milli, J., Girard, J. H., & Bonnefoy, M. 2012, *A&A*, 546, 24
 Raymond, S. N., & Armitage, P. J. 2013, *MNRAS*, 429, L99
 Rice, W. K. M., Armitage, P. J., Wood, K., & Lodato, G. 2006, *MNRAS*, 373, 1619
 Siess, L., Dufour, E., & Forestini, M. 2000, *A&A*, 358, 593
 Tannirkulam, A., Harries, T. J., & Monnier, J. D. 2007, *ApJ*, 661, 374
 Thalmann, C., et al. 2010, *ApJ*, 718, L87
 Van Boekel, R., Min, M., Waters, L. B. F. M., de Koter, A., Dominik, C., Van den Ancker, M. E., & Bouwman, J. 2005, *A&A*, 437, 189
 Verhoeff, A. P., et al. 2011, *A&A*, 528, 91
 Wetherill, G. W. 1980, *ARA&A*, 18, 77
 Zhu, Z., Nelson, R. P., Hartmann, L., Espaillat, C., & Calvet, N. 2011, *ApJ*, 729, 47